Title

Age Associated Increase in Microglia Inflammation and Phagocytosis in the Adult Neural Stem Cell Niche.

Authors

Ronald Cutler[1,=], Samuel Harrison[1,=], Natalia Sandoval-Kuhn[1], Stephen Tomlinson[2], Erzsebet Kokovay[1]

Affiliations

[1] UTH-SA, Department of Cell Systems and Anatomy, San Antonio, TX, USA

[2] Medical University of South Carolina, Department of Pharmacology and Immunology, Charleston, SC, USA

[=] Authors contributed equally to this work

[*] Correspondence to E.K. (KokovayE@uthscsa.edu)

Summary

Neurogenesis occurs throughout life but is reduced aging. We show that during aging, microglia in the Subventricular Zone become activated and display an inflammatory phenotype. We show that young SVZ microglia have reduced phagocytic capacity compared to whole brain microglia *in vitro*, suggesting that these niche microglia are specialized not to phagocytize stem cells and progenitors. However, during aging, SVZ microglia exhibit increased phagocytosis. We show that during aging, there is a significant increase in the number of microglia that have NSC and progenitor markers within the lysosomes, strongly suggesting that during aging microglia engulf NSCs and progenitors. Reducing inflammation improves proliferation but had no significant reduction on phagocytosis suggesting that inflammation is not a key driver in the age-associated phagocytosis but is important in reduced proliferation. This indicates that SVZ microglia are key regulators of neurogenesis in the aged SVZ.

41 **Introduction**

42 Adult neural stem cells (NSCs) reside in two neurogenic niches of the murine brain named the
43 subgranular zone (SGZ) of the dentate gyrus and the subventricular zone (SVZ). These NSCs give
44 rise to neurons, astrocytes, and oligodendrocytes. Neurogenesis, the production of new neurons,
45 occurs throughout life in the SVZ and SGZ niches. Here, we are focused on the NSCs in the SVZ
46 niche, which during normal brain homeostasis, are in a quiescent state (qNSCs) or actively
47 dividing state (aNSCs). aNSCs produce a progenitor cell called transit amplifying cells (TACs),
48 which proliferate multiple times to eventually yield neuroblasts. These neuroblasts migrate from
49 the SVZ through the rostral migratory stream (RMS) and into the olfactory bulb (OB), where they
50 mature and integrate into the neuronal circuitry of the OB (Alvarez-Buylla and García-Verdugo,
51 2002). During aging, there is a drastic decline in the proliferation of NSCs, increased NSC
52 quiescence, and reduced NSC number (Ahlenius et al., 2009; Enwere et al., 2004; Kalamakis et
53 al., 2019; Maslov et al., 2004; Solano Fonseca et al., 2016).

54 Microglia, the innate immune cells of the brain, function as monocytes and extend processes for
55 surveillance of the local tissue. Microglia are myeloid progenitors that originate in the yolk sac
56 and infiltrate the CNS during development, which comprise around 10% of the cell population of
57 the adult brain (Ginhoux et al., 2010). Microglia are versatile cells that work to clear cellular debris
58 or dying cells via phagocytosis, produce signaling molecules to maintain brain homeostasis,
59 maintain neuronal synapses by synaptic pruning, and help to repair tissue following injury
60 (Colonna and Butovsky, 2017). It has been observed that microglia that reside in the SVZ niche
61 have distinct properties from other brain regions in morphology, ability to support NSC
62 proliferation and neurogenesis (Goings et al., 2006; Marshall et al., 2014; Ribeiro Xavier et al.,
63 2015; Shigemoto-Mogami et al., 2014; Solano Fonseca et al., 2016). However, we have previously

64 observed that during aging SVZ microglia become more activated and proinflammatory. In fact,
65 age-related increase in SVZ microglial activation precedes the decline of NSC proliferation,
66 suggesting that microglia activation may be a driver of NSC dysfunction (Solano Fonseca et al.,
67 2016). Here, we found that during aging, SVZ microglia not only display significant upregulation
68 of pro-inflammatory signatures, but also show increased lysosomal marker and morphology of
69 activatation. We show that SVZ microglia become more phagocytic during aging i*n vitro* and *in*
70 *vivo*, where they engulf aNSCs and TACs and express more inflammation associated genes.
71 Finally, we performed interventions to reduce inflammation and saw a partial rescue of both
72 proliferation and TAC number, however this was not accompanied by a reduction in TAC
73 phagocytosis, suggesting that microglia inflammation contributes to reduced NSC proliferation
74 but is not a driver of NSC phagocytosis during aging.

75 **Age-related changes in SVZ microglia morphology**

76 We have previously shown that SVZ neurogenesis is reduced by 12 months of age (Solano
77 et al., 2016). To understand how SVZ microglia change during aging, we performed
78 immunohistochemistry for the microglia marker Iba1 and the lysosomal marker CD68 in the SVZs
79 dissected as wholemounts to preserve the 3-D cytoarchitecture of the niche, from 3- and 12-month-
80 old mice. In young adult mice (3-month-old), we observed ramified cell morphology throughout
81 the SVZ indicated by Iba1+ signal with relatively low amounts of CD68+ signal within Iba1+ cells
82 (Fig. 1A). In aged mice (12-month-old), we observed a more activated cell morphology with fewer
83 processes, larger cell bodies, and higher amounts of Cd68+ signal within Iba1+ microglia in the
84 SVZ (Fig. 1C). During neuronal development, it has been shown that microglia adopt a phagocytic
85 phenotype, reminiscent of the phenotype seen during SVZ aging, and was associated with

86 phagocytosis of precursor cells during development. This led us to hypothesize that activated
87 microglia in the aging SVZ may also have increased phagocytotic activity.

88

89

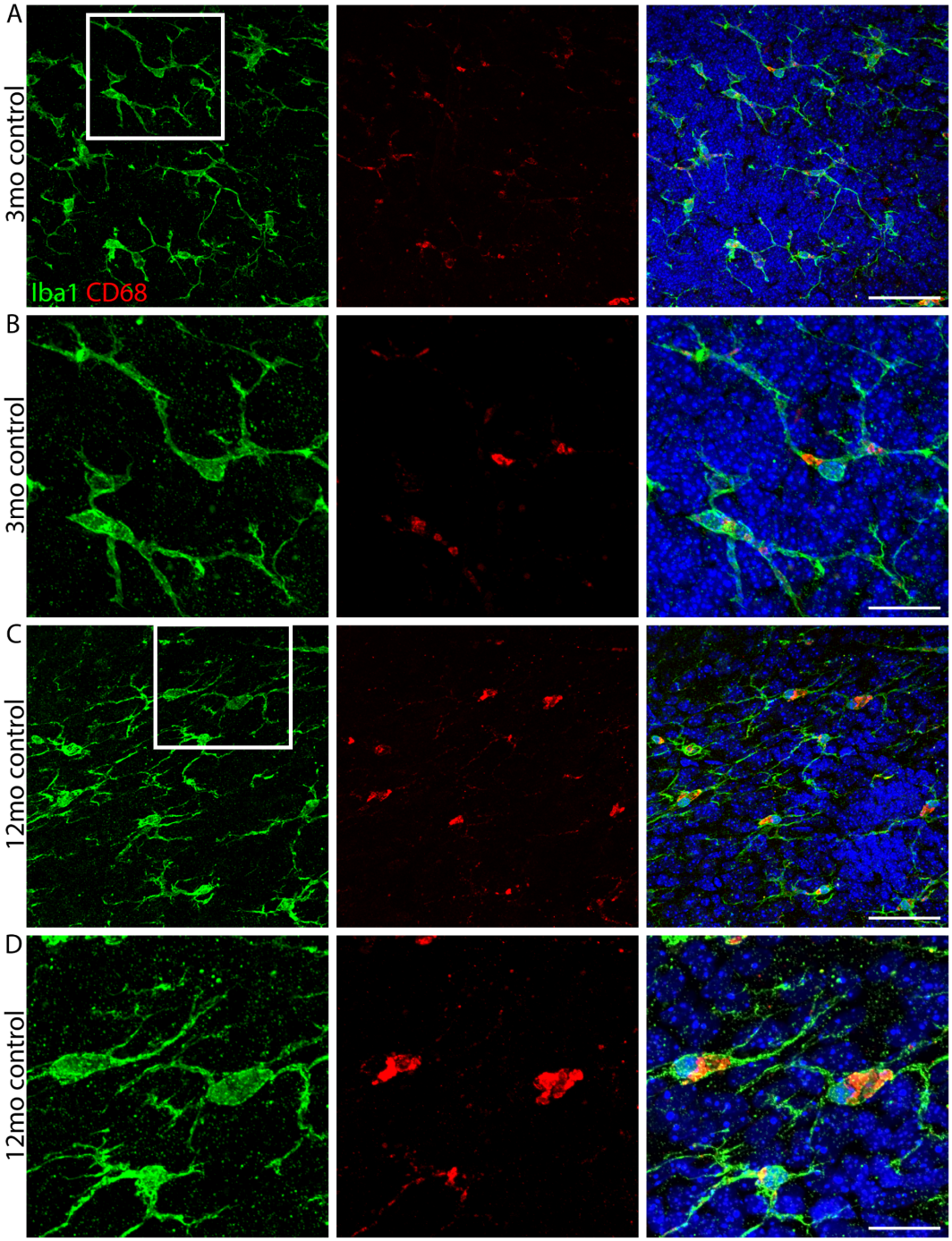

Figure 1. Age-Associated SVZ Microglia Morphological Changes and Increased Activation. Representative confocal projection images of SVZ microglia stained with Iba1 (*green*) and microglia lysosomes stained with CD68 (*red*). (A) Young (3-month) SVZ microglia imaged at 40x magnification. Scale bar: 50µm. (B) Young SVZ microglia imaged at 100x magnification. Scale bar: 20µm. (C) Aged (12-month) SVZ microglia imaged at 40x magnification. Scale bar: 50µm. (D) 12-month SVZ microglia imaged at 100x magnification. Scale bar: 20µm.

97 **Gene expression in the aging SVZ suggest increased phagocytosis of NSCs by microglia**

98 To determine if there are age-related transcriptional changes in SVZ microglia as well as
99 NSCs related to phagocytosis and inflammation, we reanalyzed a published data set that profiled
100 14,685 single-cell transcriptomes from the SVZ of young (3-month-old) and old (28/29-month-
101 old) male mice. With this, we created pseudobulk samples for each cell type and biological
102 replicate and performed differential gene expression (DGE) analysis to compare old vs. young,
103 followed by gene set enrichment analysis (GSEA) (Supplemental Fig. 1). We first focused on the
104 age-related changes in the microglia, where we found 254 and 54 genes significantly (adjusted p-
105 value < 0.05) up- and down-regulated, respectively (Supplemental Fig. 1C). GSEA of the
106 upregulated genes revealed processes involved in translation and secretion of inflammatory
107 cytokines, and lipid metabolism, which has been previously reported (Yen et al., 2024). GSEA of
108 downregulated genes revealed processes involved in cytoskeleton organization, which has not
109 been reported before and may suggest dysfunction in migration (Supplemental Fig. 1D).

110 Notably, we did not find enrichments of phagocytosis from GSEA, however, we did find
111 genes that act as receptors for phagocytosis, such as *Axl* and *Tlr2*, to be amongst the genes with
112 the highest increase in gene expression during microglia aging (Supplemental Fig. 1C). Thus, we
113 curated comprehensive gene sets related to several aspects of phagocytosis from the molecular
114 signatures database (Liberzon et al., 2024) and overlapped these with the set of age-related
115 differentially expressed genes (ARDEGs; adjusted p-value < 0.05). Out of 19 genes related to
116 phagocytosis that overlapped with the microglia ARDEG set, 18 were found to be significantly
117 upregulated in old microglia as compared to the young (Fig. 2A). Notably, 8 of these genes (*Cyba,*
118 *Atp6v0e, Rab7b, Cybb, Vim, B2m, Tlr2,* and *Hvcn1*) were associated with the formation of
119 phagocytic vesicles. We extended our phagocytosis gene set to include genes identified through

120 screens from previous studies (Haney et al., 2018), (Pluvinage et al., 2019), and found that all 9
121 genes that overlapped with the microglia ARDEGs were significantly upregulated in old microglia
122 as compared to the young (Supplementary Figs. 2A,B). However, it is possible that the
123 upregulation of these genes may be part of a compensatory response to the increase in phagocytic
124 activity. In the same vein, we found that the expression of the receptor essential for microglial
125 function, *Csf1r*, was downregulated in aged microglia while the ligand *Csf1* showed the opposite
126 trend and thus may be a compensatory response to chronic microglia activation (Hu et al., 2024)
127 (Supplementary Fig. 2C). Finally, we found that the broad upregulation of phagocytosis-related
128 gene expression was also accompanied by an increase in the expression of genes related to
129 microglia activation (Supplementary Figs. 2C-D). Overall, these findings suggest that aging causes
130 complex gene expression reprogramming which shifts the expression profiles of aged microglia to
131 resemble those in the states of phagocytosis, activation, and development (Izgi et al., 2022). This
132 is further supported by the phenotypic resemblance of aged SVZ microglia to microglia in the
133 developmental context in terms of an activated morphology and increased phagocytosis of neural
134 progenitors (Cunningham et al., 2013).

135 We next asked if the upregulation of phagocytosis-associated gene expression was specific
136 to any of the known cell surface receptors pathways required for this process. By using a curated
137 list of the components of each receptor pathway known to be associated with phagocytosis, we
138 found gene expression upregulation of the receptors in the Complement, TAM, and Toll-like
139 pathways. On the other hand, for the FC gamma, Scavenger, P2ry6, and Trem2 receptor pathways,
140 we found largely consistent upregulation of gene expression for the components of these pathways,
141 which did not coincide with upregulation of the core receptor (Deczkowska et al., 2018).Of note,
142 while we did not detect increased expression of the receptor Trem2 in aged microglia, which is

143 known to promote anti-inflammatory responses and phagocytosis, we did find an expression
144 pattern in aged microglia consistent with the disease-activated microglia (DAM) stage 2 signature
145 that has been reported to be Trem2-dependent (Supplementary Figs. 2E). Overall, these results
146 suggest that during the aging of microglia, there is a complex upregulation of expression for genes
147 across multiple phagocytosis pathways that corresponds with a unique Trem2-independent DAM
148 state

149 We then turned our attention to analyzing the transcriptomes of the neural progenitor cells
150 where we asked if we could detect any age-related expression changes in genes related to target
151 cell engulfment, such as apoptosis, "find-me," "eat-me," and "don't eat-me" signals. Compared to
152 microglia, there were very few ARDEGs, as only 13 genes were found to be significantly (adjusted
153 p-value < 0.05) upregulated in aged Astrocyte-qNSC as compared to young, while none were
154 identified in aged aNSC, TACs or Neuroblasts when compared to young (Supplementary Figs. 1E-
155 J). Because of the lack of significant ARDEGs, instead of overlapping gene sets of interest with
156 the ARDEGs for each of the neural progenitor cell types, we utilized GSEA, as this method does
157 not rely on setting significance thresholds and considers changes of sets of genes rather than
158 individual genes (Methods). We paired this approach with curated gene sets that contained genes
159 associated with apoptosis, "find-me," "eat-me," and "don't eat-me" signals (Supplementary Table
160 2). With this, we found a significant (adjusted p-value < 0.05) age-related upregulation of the
161 expression of the apoptosis gene set in Astrocyte-qNSC cells, which contrasted with an age-related
162 decrease in aNSC, TACs and Neuroblasts (Fig. 2C; Supplementary Fig. 3A). Although we were
163 unable to find any significant enrichments when using genes sets for "find-me" or "eat-me"
164 signals, we did find significant age-related upregulation of the expression for complement system
165 and opsonization gene sets (known to be associated with "eat-me" signals (Li, 2012)) in Astrocyte-

166 qNSC and Neuroblasts, but not in aNSC or TACs (Fig. 3C; Supplementary Fig. 3B-C).
167 Intriguingly, we also found significant age-related upregulation of the expression for the "don't
168 eat-me" gene set in Astrocyte-qNSC and Neuroblasts but not in aNSC-NPCs (Fig. 2C;
169 Supplementary Fig. 3D). The "don't eat-me" gene set includes genes that are part of the MHC
170 Class I complex, as they are known to function as a "don't eat-me signal" against macrophages in
171 certain contexts, especially when co-expressed with the *B2m* subunit (Khalaji et al., 2023).
172 Importantly, the receptor of MHC I, *Lilrb4a*, is among the genes whose expression is significantly
173 upregulated in aged microglia (Supplementary Fig. 1C). Because of this, we also looked for age-
174 related expression changes using the antigen processing and presentation gene set (MHC pathway).
175 The expression pattern of this gene set matched the trends of the "don't eat-me" gene set, which is
176 suggestive of anti-phagocytic function of the MHC Class I complex in aged Astrocyte-qNSC and
177 Neuroblasts, but not aNSC-NPCs. In summary, while all 3 neural progenitor cell types have
178 increased expression of complement system genes that are associated with "eat-me" signals and
179 thus may promote phagocytosis, Astrocyte-qNSC and Neuroblasts appear to counteract this signal
180 through increased expression of "don't eat-me" signals such as *Cd200, Pecam1*, and the MHC
181 class 1 complex (*H2-K1, H2-D1, B2m*). This suggest that the age-related increase in phagocytic
182 activity of microglia may be targeted towards aNSC and TACs.

183

184

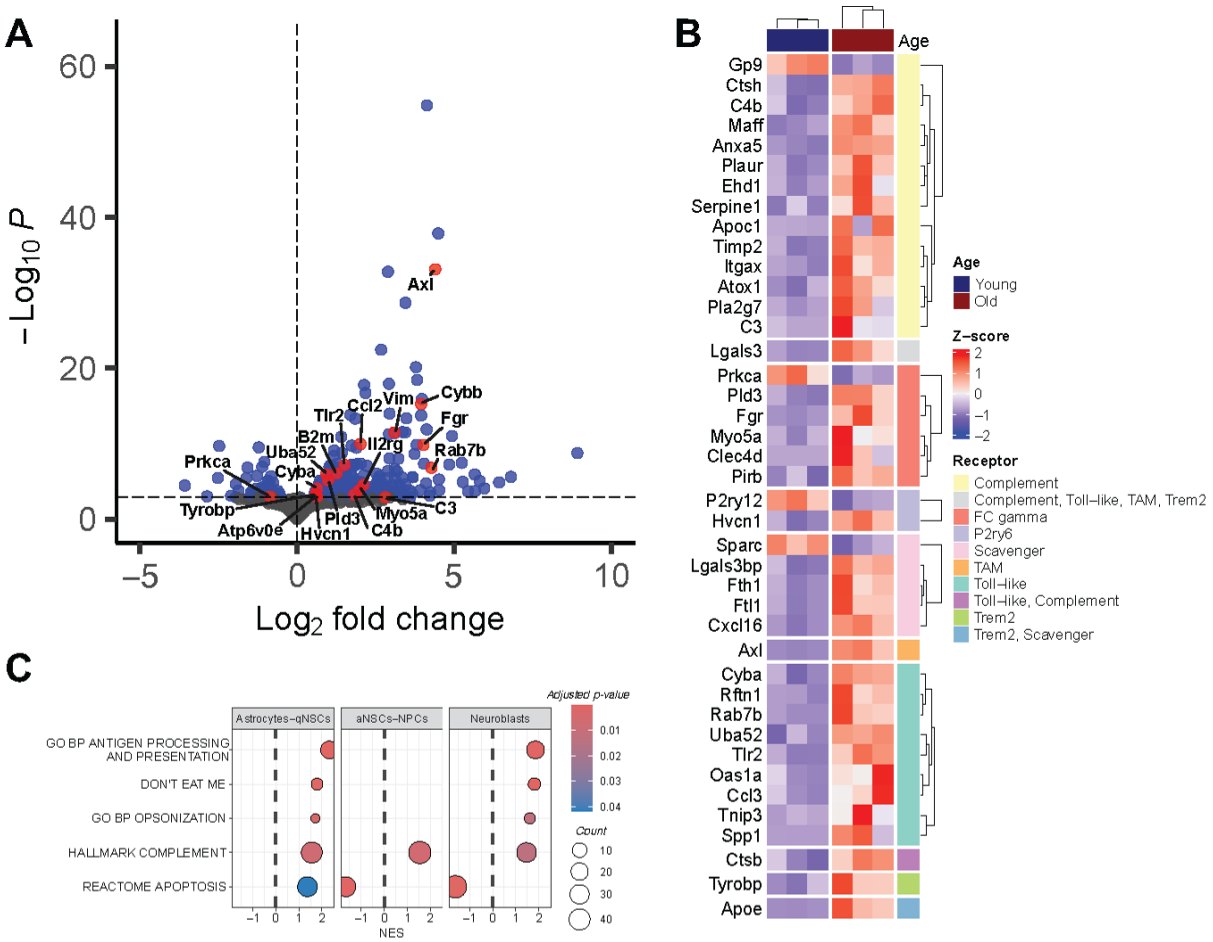

Figure 2. Re-analysis of aging SVZ scRNA data reveals age-related increase of microglia phagocytosis.
(A) Pseudobulk level analysis of differential gene expression (DGE) changes during aging of young (3 months old) and aged (28–29 months old) microglia in the SVZ. Red points genes that overlapped with the phagocytosis-related gene sets (Supplementary table 2) and are log2 fold change > 1 and adjusted p-value < 0.05. Statistics: n=3 mice/group, DGE results obtained using Wald test followed by Benjamini-Hochberg correction for multiple hypothesis testing. (B) Heatmap of age-related DEGs (adjusted p-value < 0.05) in aging SVZ microglia (obtained from analysis in (A)) that overlapped with phagocytosis-related gene sets (Supplementary table 2) Statistics: n=3 mice/group. (C) Gene set enrichment analysis of age-related gene expression changes in neural progenitor cells using apoptosis, "find-me," "eat-me," and "don't eat-me" signal gene sets (Supplementary table 2). Statistics: n=3 mice/group, GSEA p-values obtained using a permutation test followed by followed by Benjamini-Hochberg correction for multiple hypothesis testing.

200

201 **Microglia in the SVZ have an age-related increase of hagocytosis of NSCs and TACs**

202 To assess SVZ microglia phagocytic activity, we dissected out the SVZ from the brain of
203 mice, isolated microglia from either the SVZ or whole brain (excluding the SVZ) from 3- and 12-
204 month old mice (young and old), and then expanded them *in vitro* where engulfment of yeast
205 particles conjugated to pHrodo, a pH sensitive dye (Kapellos et al., 2016), was measured via live
206 imaging (Methods). Interestingly, we observed relatively low phagocytic activity in the 3-month-
207 old SVZ microglia compared to 3-month old microglia isolated from the whole brain, suggesting
208 that microglia in the SVZ niche are specialized to be less phagocytic than non-germinal areas in
209 the brain. However, microglia from 12-month-old SVZ showed a significant age-related increase
210 in phagocytosis activity compared to the 3-month-old SVZ microglia, which approached levels of
211 phagocytic activity of microglia isolated from whole brain (Fig. 3A).

212 Next, we sought to validate the findings of an age-related increase in SVZ microglia
213 phagocytosis activity in our *in vitro* system by examining SVZ microglia phagocytosis *in vivo*.
214 First, we asked if age-associated increases in microglia lysosomal activity in the SVZ was due to
215 increased phagocytosis of apoptotic NSCs and TACs. We performed immunohistochemistry for
216 cleaved caspase 3 on coronal sections from 3-month-old and 12-month-old mice. We did not
217 observe a significant increase in apoptosis in the aged SVZ (Fig.3B) Next, to detect if phagocytosis
218 increased during aging, we performed immunohistochemistry (IHC) on SVZ wholemounts against
219 the microglia marker Iba1, lysosome marker CD68, and the aNSC/TAC marker Mash1 (Kim et
220 al., 2011; Lim and Alvarez-Buylla, 2016). Interestingly, we observed colocalization of the
221 lysosome marker CD68 and Mash1 within microglia in both 3- and 12-month-old SVZs (Fig. 3C

222 &D). Quantification revealed approximately 20% of SVZ microglia contain Mash1 within their

223 lysosomes in 3-month-old SVZ, which significantly increased by 12 months of age (Fig. 3C).

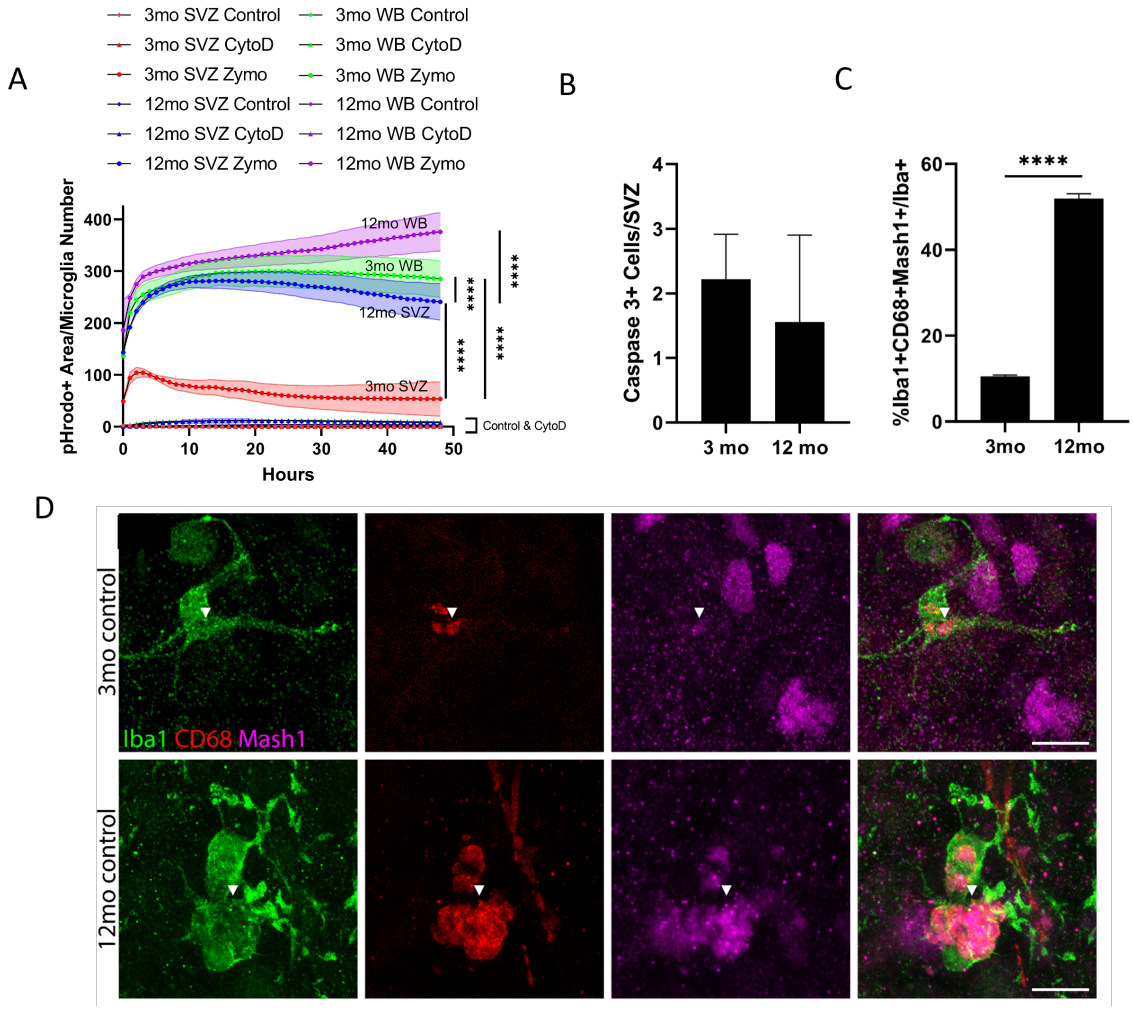

224

225 **Figure 3. Age-related increase in SVZ microglia phagocytosis *in vitro* and *in vivo*. (A)** Time-
226 lapse *in vitro* phagocytosis assay of young (3-month) or aged (12-month) SVZ or whole brain
227 (WB) microglia labeled with isolectin and incubated with Zymosan-pHrodo (Zymo),
228 CytochalasinD and Zymosan-pHrodo (CytoD), or isolectin only (Control). Phagocytosis is
229 quantified as pHrodo+ area indicated by red fluorescence / microglia number. Statistics: n=3
230 mice/group, microglia > 1,000 per mouse. (B) Quantification of Caspase 3 in coronal brain
231 sections. Statistics: n=6 mice/group. (C) Quantification of *in vivo* phagocytosis of 3- or 12-month
232 SVZ microglia measured as Iba1+CD68+Mash1+ microglia / total Iba1+ microglia. *n*=11
233 mice/group. (D) Representative confocal projection images of young or aged SVZ microglia
234 stained with Iba1 (*green*), microglia lysosomes stained with CD68 (*red*), and TAC transcription
235 factor stained with Mash1 (*magenta*). Scale bar: 10µm. P-value legend: ns: no symbol; *: $p \leq 0.05$,
236 **: $p \leq 0.01$, ***: $p \leq 0.001$, ****: $p \leq 0.0001$.

237 **CR2-crry complement 3 intervention increased NSCs proliferation but not phagocytosis**

238 To identify possible mechanisms for the age-related increase in microglia phagocytosis of
239 aNSC/TAC in the SVZ, we performed qRT-PCR for pro-inflammatory genes shown to be
240 upregulated in microglia during aging from our analysis of RNAseq databases. We reasoned that
241 pro-inflammatory genes that are very low or absent in the young SVZ compared to microglia
242 isolated from outside the SVZ that are increased with age in SVZ microglia would be good
243 candidates based on our *in vitro* phagocytosis results. One gene identified to be higher in microglia
244 isolated from outside the germinal region compared to young SVZ microglia, that was highly
245 upregulated upon aging was Complement 3 (C3) (Fig. 2, Supplementary Fig. 4). We found that
246 receptors for C3, *ITGAM* (Complement receptor 3), and *ITGAX* (Complement receptor 4) were
247 upregulated in SVZ microglia during aging (Supplementary Fig 4). To inhibit C3 activity we
248 utilized CR2-crry, a protein developed for targeted inhibition of C3 cleavage and C3 deposition
249 (Atkinson et al., 2005; Song et al., 2003). 3- and 12-month-old mice (young and old) mice received
250 CR2-crry or saline treatment every other day for a total of 3 doses followed by an EdU pulse 2
251 hours before sacrifice to label proliferating cells (Fig. 4A). SVZ wholemounts were collected and
252 IHC was performed as described above .

253 CR2-crry treatment had no significant effect on proliferation (Fig. 4F), SVZ microglia
254 CD68 area (Fig. 4B), or SVZ microglia phagocytosis of TACs (Fig. 4G) in the SVZs isolated from
255 3-month-old mice. We observed an expected decline in SVZ proliferation from 3- and 12-month-
256 old saline treated mice (Fig. 4F). There was a significant increase in SVZ proliferation in 12-
257 month-old CR2-crry treated groups compared to 12-month-old saline treated groups indicated by
258 EdU+ cells (Fig. 4F). We observed an increase in CD68 area/Iba1+ cells in 12-month-old saline
259 treated groups compared to 3-month-old saline treated groups (Fig. 4B), with a non-significant

260 decrease in 12-month-old CR2-crry treatment CD68 area/Iba1+ cell compared to 12-month-old
261 controls (Fig. 4B). There was an increase of Iba1+CD68+Mash1+ colocalization within Iba1+ cells
262 in 12-month-old saline treated controls compared to 3-month old saline treated controls (Fig. 4G)
263 with an increase of Iba1+CD68+Mash1+ colocalization within Iba1+ cells in 12-month-old CR2-
264 crry treatment vs 12-month-old controls (Fig. 4G). These findings suggest that C3 is involved in
265 age-related declines in proliferation but not aNSC and TAC phagocytosis. The increase in
266 phagocytosis of aNSCs and TACs during aging suggests that increasing the number of aNSCs and
267 TACs produced via cell division results in more cells being present to undergo phagocytosis.

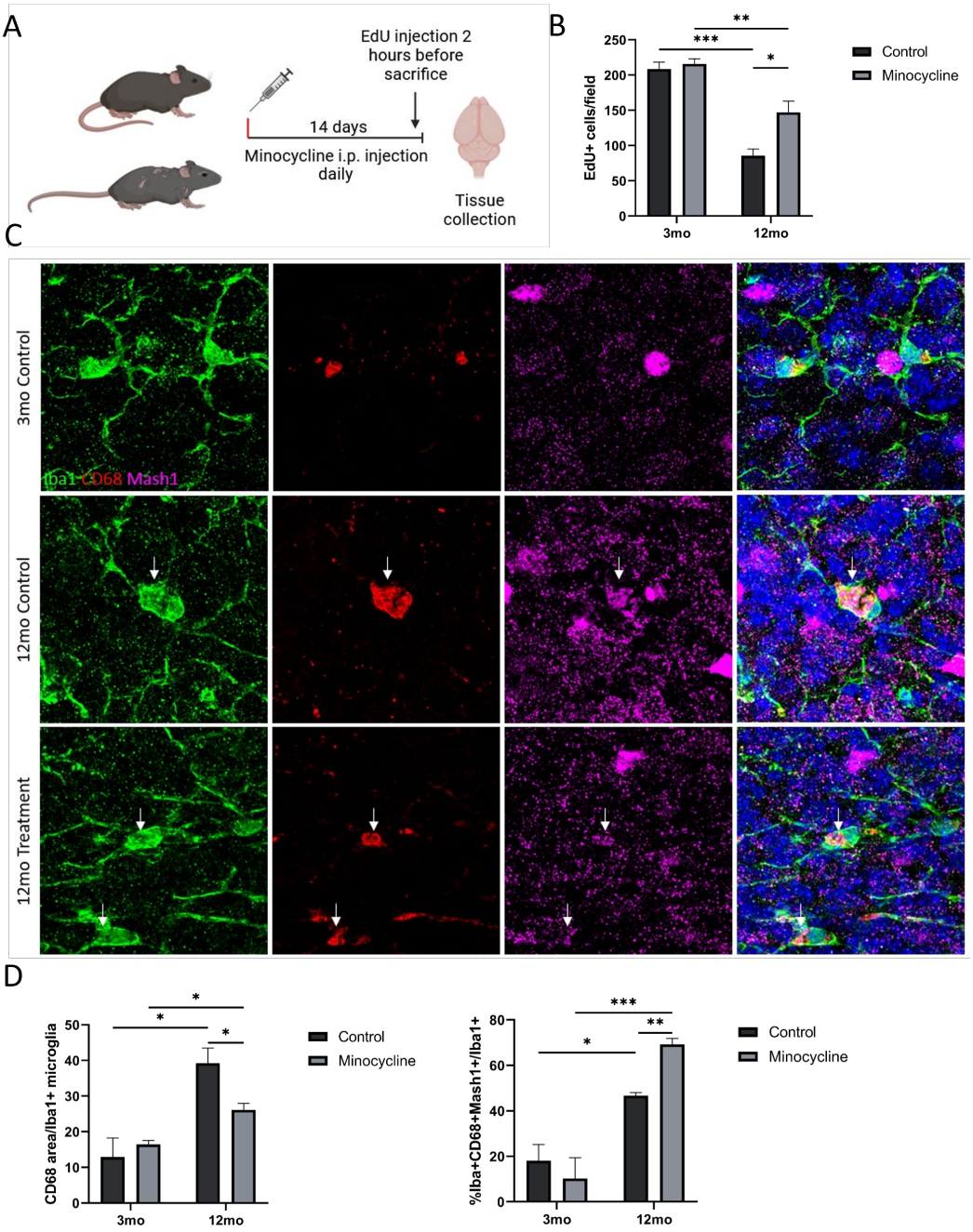

Figure 4. Minocycline treatment restores some proliferation in the aged SVZ but does not reduce SVZ microglia phagocytosis. (A) Graphic representation of experimental design. (B) Quantification of EdU positive cells in the SVZ of young (3-month) or aged (12-month) mice. (C) Confocal micrographs the SVZ from young vehicle treated, old vehicle treated and minocycline treated mice. (D) Quantification of CD68 area Iba1+ microglia n=5 mice/group. (E) Quantification of percent Iba+ Mash1+ CD68+ cells n=5mice/group. P-value legend: ns: no symbol; *: $p \leq 0.05$, **: $p \leq 0.01$, ***: $p \leq 0.001$, ****: $p \leq 0.0001$.

276 **Minocycline anti-inflammatory intervention effects on SVZ microglia and NSCs**

277 We have previously seen that SVZ microglia have high levels of activation with increased
278 CD68 compared to non-germinal regions during aging, resulting in a pro-inflammatory milieu in
279 the SVZ (Solano Fonseca et al., 2016). We wanted to determine if broadly reducing the activation
280 of aged SVZ microglia would result in increased proliferation and/or reduced phagocytosis. We
281 treated 3- and 12-month old mice (young and old) mice with minocycline, an antibiotic with potent
282 anti-inflammatory properties (Elewa et al., 2006; Garrido-Mesa et al., 2013; Plane et al., 2010;
283 Tikka et al., 2001; Yrjänheikki et al., 1998) or saline for 14 days followed by a 2 hour EdU pulse
284 to label proliferating cells (Fig. 5A) before euthanasia. SVZ wholemounts were collected for
285 immunohistochemistry as previously described. At 3 months of age, minocycline treatment did not
286 have a significant effect on microglial CD68 expression (Fig. 5B), proliferation (Fig. 5F), or SVZ
287 microglia phagocytosis of Mash1 positive cells (Fig 5G). At 12 months of age, minocycline
288 treatment resulted in a significant reduction in microglia expression of CD68 compared to saline
289 treated controls (Fig. 5B), indicating that minocycline reduced inflammation in the aged SVZ.
290 Minocycline treatment resulted in increased proliferation in the aged SVZ (Fig. 5F) although this
291 did not reach levels measured in young mice. As expected, we saw a significant increase in the
292 number of CD68 positive lysosomes containing Mash1 in the 12-month-old SVZs compared to
293 young 3-month-old SVZs (Fig. 5G). Surprisingly, we observed a significant increase in Mash1
294 containing lysosomes in the SVZs of 12-month-old mice treated with minocycline compared to
295 saline treated controls (Fig. 5G), indicating that anti-inflammatory treatment alone does not reduce
296 phagocytosis in the SVZ.

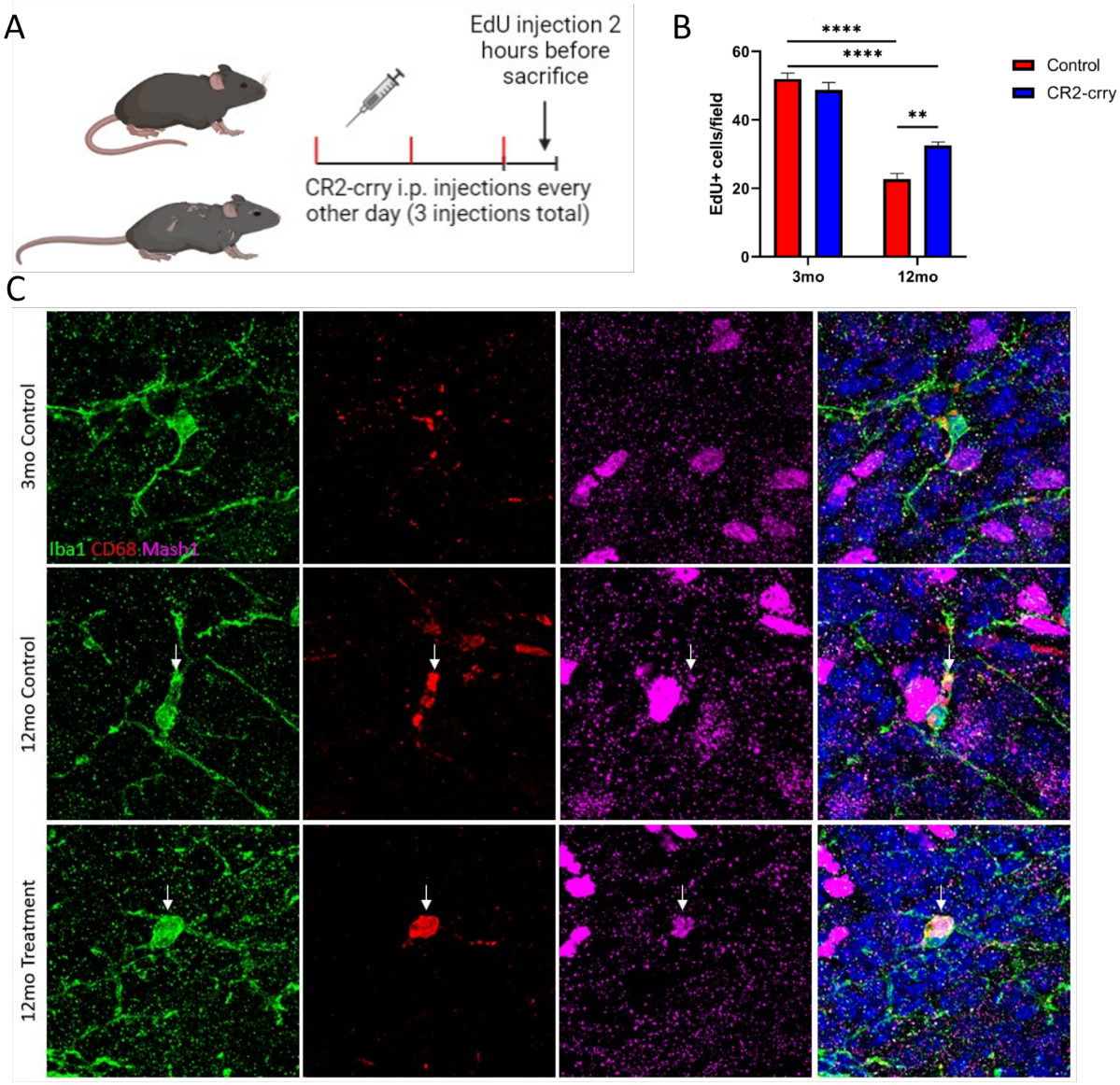

Figure 5. Complement inhibition partially rescues SVZ proliferation in aged mice and further increases SVZ microglia phagocytosis. (A) Graphic representation of CR2-crry or saline administration to young (3-month) or aged (12-month) mice. (B) Quantification of microglia activation measured by CD68 area / number of microglia. (C) Confocal projection images of young control, aged control, aged CR2-crry treated SVZ microglia stained with Iba1 (*green*), microglia lysosomes stained with CD68 (*red*), and TAC transcription factor stained with Mash1 (*magenta*). Arrowheads in aged control and aged CR2-crry treated indicate colocalization of Mash1+ signal within microglia lysosomes (Iba1+CD68+). Scale bar: 10µm. (D) Quantification of proliferating EdU-positive cells in the SVZ of young or aged control or CR2-crry treated mice. (E) Quantification of Mash1 containing microglia measured by Iba1+CD68+Mash1+ / number of Iba1+ cells from young or aged control or CR2-crry treated mice. *n*=4 mice/group. P-value legend: ns: no symbol; *: $p \leq 0.05$, **: $p \leq 0.01$, ***: $p \leq 0.001$, ****: $p \leq 0.0001$.

310 **Discussion**

311 The adult SVZ produces new neurons for the distant olfactory bulb throughout life which
312 contribute to olfactory learning and discrimination (Lledo and Vally 2016). In addition, following
313 brain injury neural progenitors and neuroblast undergo a proliferative burst and then migrate to
314 damaged areas where they give rise to a limited number of neurons, astrocytes and
315 oligodendrocytes and secrete pro-reparative factors (Liang…Carmichael 2019, Yamashita 2006 J
316 Neuro, Imotola 2004, Robin, 2006). The blockade of this response results in larger legions and
317 worsens behavioral deficits (Carmichael Ohab 2006). This reparative ability makes the SVZ an
318 enticing therapeutic target to boost the endogenous repair response. During aging SVZ
319 neurogenesis becomes drastically reduced with the most-rapid reductions between 9-12 months of
320 age in the rodent (Luo…Conover 2006 Aging Cell) corresponding to middle-age and persists for
321 the duration of aging. The reduction is coincidental to periods of increasing risk for brain injury
322 associated with aging. Thus, understanding drivers of SVZ NSC age-associated dysfunction is
323 imperative. Our findings indicate that pro-inflammation and upregulation of phagocytotic
324 signatures within the SVZ niche by microglia plays a role in decreased NSC number and reduced
325 proliferation reported during aging.

326 During embryonic neurogenesis, SVZ microglia have ameboid morphology and regulate
327 the size of the precursor pool by phagocytosis of non-dying neuroblasts (Cunningham et al., 2013;
328 Morrison et al., 2023) In the adult dentate gyrus, another neurogenic niche, unactivated microglia
329 phagocytose newborn neurons undergoing apoptosis In contrast, in the adult SVZ, very little
330 apoptosis occurs (Luo et al., 2006). In contrast, in the olfactory bulb where newborn neurons
331 generated in the SVZ must integrate into the circuitry widespread phagocytosis has been reported
332 (Xavier et al., 2015). Using immunohistochemistry, we did not observe an increase in apoptosis in

333 the aging SVZ suggesting that the observed increased phagocytosis of aNSCs/TACs was not due
334 to increased phagocytosis.

335 Microglia are distributed throughout the brain, however there are regional differences that
336 make them heterogenous within their local microenvironment such as differences in cell density,
337 morphology, transcriptomes, and receptor expression (Grabert et al., 2016; Tan et al., 2020). SVZ
338 microglia have distinct characteristics compared to microglia from non-germinal regions
339 indicating the specialization of microglia within the SVZ niche (Marshall et al., 2014; Ribeiro
340 Xavier et al., 2015; Shigemoto-Mogami et al., 2014; Solano Fonseca et al., 2016)..Riberio Xavier
341 et al. reported that SVZ microglia in young adult mice not only have a distinct morphological
342 phenotype, but also have specialized gene and receptor expression compared to microglia
343 distributed in non-germinal regions. They also showed the necessity of SVZ microglia for
344 neuroblast survival and migration from the SVZ; while suggesting that SVZ microglia perform
345 little amounts of phagocytosis within the young SVZ niche, possibly because of low expression of
346 the P2Y12 receptor (Ribeiro Xavier et al., 2015). We found that young SVZ microglia *in* vitro
347 exhibit less phagocytosis then microglia from other brain regions which supports the notion that
348 they are specialized to be less phagovcytic in the young SVZ microenvironment.

349 To understand the roles of the observed age-associated increase in SVZ microglia
350 phagocytosis on aging NSCs of the SVZ, we utilized minocycline and CR2-crry in vivo
351 interventions to reduce SVZ microglia inflammation and phagocytosis respectively. Due to the
352 high levels of microglia activation in the SVZ, minocycline treatment was used to investigate if a
353 decrease in microglia inflammation in the aged SVZ would rescue NSC proliferation and/or result
354 in a decrease of TAC phagocytosis. Minocycline is often used as a general anti-inflammatory, that
355 has been shown to offer neuroprotection and reduces the activation of microglia (Ekdahl et al.,

356 2003; Plane et al., 2010; Tikka et al., 2001; Wu et al., 2002; Yrjänheikki et al., 1998). CR2-crry
357 treatment, a murine C3 activation and deposition inhibitor (Atkinson et al., 2005; Song et al., 2003)
358 that crosses the blood brain barrier (Alawieh et al., 2018), was used to selectively inhibit C3 of the
359 complement pathway. With minocycline treatment we observed a significant decrease in SVZ
360 microglia activation in the 12-month-old treated mice, indicating that minocycline was reducing
361 inflammation in the aged SVZ. Importantly, the aged mice that received minocycline had an
362 increase in SVZ proliferation, indicating that the age-associated decline of SVZ proliferation can
363 be partially rescued by the administration of minocycline. Similar to the minocycline results, CR2-
364 crry intervention in aged mice resulted in a trending decline in SVZ activation as well as an
365 increase in SVZ proliferation. Suggesting that treating aged mice with CR2-crry not only reduced
366 microglia activation in the SVZ but also partially rescued the age-associated decline of SVZ
367 proliferation in a complement mediated fashion. Both in vivo interventions had strikingly similar
368 results. including an increase in SVZ microglia phagocytosis of aNSCs and TACs in the aged
369 groups treated with either minocycline or CR2-crry. With both interventions we saw a further
370 increase in aNSCs and TAC phagocytosis. The increase in microglia phagocytosis observed in the
371 12 month treated mice occurred in the presence of increased SVZ proliferation, which has not been
372 previously described. Our findings suggest, based on the increase in number of proliferating SVZ
373 cells, that SVZ microglia inflammation is responsible at least in part for the age-related reduction
374 in neurogenesis. However, the increases seen in SVZ microglia phagocytosis suggest that more
375 cells in the aged SVZ further increases phagocytosis. This could be potentially due to the increase
376 of cells within the SVZ expressing “eat me” signals without upregulation of the “don’t eat me”
377 signals that were associated with qNSCs and neuroblasts, which was detected in our analysis of
378 the available RNAseq data. An increase in cells that express “eat me” signals will be an important

379 future direction to explore as a possible mechanistic answer to our observed age-associated
380 increase in SVZ microglia phagocytosis.

381

382 **Methods**

383 Animals and Interventions

384 Male and female C57BL/6 mice were used in this study either bred at the UTHSA vivarium or
385 acquired from the National Institute of Aging. Young mice (2-4 months of age) and aged mice (12-
386 14 months of age) were housed in accordance with the University of Texas Health San Antonio
387 Institutional Animal Care and Use Committee and performed in accordance with institutional and
388 federal guidelines and allowed free access to water and standard rodent chow ad libitum.

389 Both male and female C57BL/6 mice (2-4 months or 12-14 months) received CR2-crry (10µg/1g
390 mouse; Stephen Tomlinson Lab, Medical University of South Carolina) or minocycline (50µg/1g
391 mouse; Sigma-aldrich, Cat. No. M9511) with respective saline controls via intraperitoneal
392 injection. Minocycline or saline was administered daily for 2 weeks. CR2-crry or saline was
393 administered every other day for a total of 3 doses.

394

395 Immunohistochemistry

396 The SVZ was isolated for wholemount (WM) tissue analysis; mice were anesthetized with
397 isoflurane, a cervical dislocation was performed, followed by brain extraction. Brains were placed
398 into cold HIB where they were halved and the septum and hippocampus were removed, and the
399 SVZ was microdissected from the surrounding brain tissue. The SVZ WM was then fixed in fresh

400 4% paraformaldehyde (PFA) for 30 minutes. SVZ WMs were permeabilized in 2% PBST and
401 blocked overnight at 4˚ C in 10% normal donkey serum (NDS). The SVZ WMs were then
402 incubated at 4°C for 4 days with primary antibody in blocking solution, followed by overnight
403 incubation at 4°C with secondary antibody made in blocking solution, and a 5-minute incubation
404 at room temperature (RT) with DAPI (1:1000; Invitrogen, Cat. No. D1306) then mounted on a
405 slide in ProLong Gold antifade reagent (Invitrogen, Cat. No. P36930). Primary antibodies that
406 were used include Iba1 (1:200; Wako, Cat. No. 019-19741 and 1:200; Novus, Cat. No. NB100-
407 1028), CD68 (1:250; BioRad, Cat. No. MCA1957), and Mash1 (1:5000; CosmoBioUSA, Cat. No.
408 SK-T01-003) Cleaved caspase 3 (1:200 Cell Signaling Cat. No D175 5A1E). Species-specific
409 secondary antibodies (Jackson ImmunoResearch) were used at a concentration of 1:500 in SVZ
410 WMs.

411

412 Immunohistochemistry Quantification

413 EdU was quantified in the SVZ by making a "Z Project" 2-dimensional image of the Z-stack in
414 ImageJ on 10 random fields of view and hand counting the number of EdU+ nuclei. The number
415 of microglia were quantified by hand counting Iba1+ cells, excluding cells whose cell body
416 touched the image boundary on Zen Microscopy Software (Zeiss). Total CD68 area was quantified
417 by making a "Z project" 2-dimensional image of the Z-stack, using the "Threshold" function, and
418 then the "Analyze particle" function to give total area in µm2 that was then averaged by total
419 number of microglia in each image. Total number of Iba1+ microglia were quantified similarly to
420 EdU+ cells described above. Mash1 colocalization within Iba1+ microglia were quantified by hand
421 counting in Zen Microscopy Software (Zeiss) by examining each Iba1+ microglia's lysosome
422 (CD68+) to determine if each Iba1+CD68+ microglia contained Mash1 colocalization. The

423 number of Mash1+CD68+Iba1+ microglia were then averaged to total number of Iba1+ microglia
424 in each image. There were no microglia that contained Mash1 that were not CD68+. SVZ WMs
425 were analyzed from 15µm thick Z-stacks (15 Z-stacks per WM). Confocal images were obtained
426 with a Zeiss LSM 710 confocal microscope at 40x objective.

427

428 Single-cell RNA-sequencing Quality control filtering

429 Quality control of downloaded single-cell RNA-Seq data (see Data Availability) was first
430 performed, which filtered cells where the number of genes or UMIs detected were greater or less
431 than 5 median absolute deviations (MADs) or percent mitochondria reads greater or less than 3
432 MADs, relative to all cells in the dataset. Genes were filtered if detected in less than 10 cells out
433 of all cells in the dataset. Cell identity labels were those assigned by the original analysis.

434

435 Single-cell RNA-sequencing differential expression and gene set enrichment analysis

436 Pseudobulk samples were created by summing counts of each identified cell type for each
437 biological replicate. The DESeq2 package (MI et al., 2014) was then used to perform differential
438 expression analysis to compare old vs. young groups. Following this the ClusterProfiler package
439 (G et al., 2012) was then used to perform gene set enrichment analysis (GSEA) using the gene
440 ontology biological process database.

441

442 Microglia phagocytosis gene set analysis

443 Genes associated with known phagocytosis receptors and/or pathways active in microglia were
444 manually curated by searching the Molecular Signatures Database (msigDB) and the literature (i.e.
445 Complement, Toll-like receptor, TAM receptor, Trem2 receptor, FC gamma, Pr2y6 receptor,
446 Scavenger receptor, Mannose receptor, LRP1 receptor, Galectin-3 adaptor protein, Microglia
447 Activation, Microglia Proliferation, Disease-Associated Microglia (DAM), and Microglia
448 Development). In addition, gene sets related to screens of phagocytosis regulators was obtained
449 from the literature (see Data Availability). These gene sets were then overlapped with the genes
450 that were found to be significantly differently expressed (adjusted p-value < 0.05) in the microglia
451 old vs. young comparison and plotted as a heatmap using the ComplexHeatmap package.

452

453 Neural stem cell gene set analysis

454 Genes associated with pathways known to be expressed in cells that are targeted for phagocytosis
455 were manually curated by searching the Molecular Signatures Database (msigDB) and the
456 literature (i.e. Apoptosis, Opsonization, Antigen Processing and Presentation, "eat-me," "find-
457 me," and "don't eat me"). Because of the lack of genes which were significantly differentially
458 expressed in neural stem cells (i.e. Astrocytes/qNSCs, aNSCs/NPCs and Neuroblasts) in the old
459 vs. young comparison, the ClusterProfiler package (ref) was then used to perform gene set
460 enrichment analysis (GSEA) using the manually curated gene sets. The Log_2 fold change of genes
461 within the gene sets found to be significantly enriched in age-related genes expression of neural
462 stem cells were then plotted as a heatmap using the ComplexHeatmap package.

463

464 Microglia Isolation and Cell Culture

465 Microglia were cultured in two ways, either plated following MACS for microglia specific culture
466 or through mixed glial culture. C57BL/6 mice were injected intraperitoneally with pentobarbital
467 (25µL/mouse) then perfused with cold 1x PBS. SVZ WMs or the remainder of the whole brain
468 excluding the SVZ and cerebellum, hereby referred to as whole brain (WB), were isolated
469 following perfusion. The tissues were minced and dissociated in 50U papain in DMEM/F12 at
470 37°C for 45 minutes and manually triturated and spun 3x in DMEM. SVZ and WB homogenate
471 were gently pressed through a 70µm cell strainer to remove debris. For mixed glial culture, SVZ
472 homogenate were then plated in a T25 flask coated with poly-L-ornithine (PLO) in neural growth
473 media (DMEM/F12, 5% fetal bovine serum, 1x N2, 10ng/mL EGF, and 10ng/mL bFGF) until a
474 confluent cell monolayer formed. The culture was then fed microglia proliferation media
475 (DMEM/F12, 10% fetal bovine serum, 1x N2, and 20 ng/mL GM-CSF) until microglia could be
476 seen atop the monolayer. Once microglia were present, they were shaken off from the cell
477 monolayer and the SVZ microglia could be plated for further experimentation.

478 For microglia isolated by MACS, following the cell strainer step, WB homogenate was
479 resuspended in HIB and centrifugated at 400G with no brake in 22% Percoll (Sigma-aldrich, Cat.
480 No. P4937) solution to remove myelin from the samples. The WB homogenate was then
481 resuspended in 0.5% bovine serum albumin and incubated with 10µL CD11b Microbeads (cat#
482 130-093-636) per 107 cells. The homogenate was then placed in an LS column (MiltenyiBiotec,
483 Cat. No. 130-042-401) in a QuadroMACS™ separator (MiltenyiBiotec, Cat. No. 130-090-976) to
484 allow for MACS sorting of CD11b + microglia following manufacturer protocols
485 (MiltenyiBiotec). WB microglia were plated in a 6-well plate coated with PLO/laminin (10µg/mL;
486 Sigma-aldrich, Cat. No. L2020) at 250k cells/well in microglia expansion media (DMEM/F12,
487 100 µg/mL PenStrep, 5 µg/mL n-acetyl-L-cysteine, 5 µg/mL Insulin, 100 µg/mL apo-transferrin,

488 100 µg/mL sodium selenite, 1 µg/mL heparin sulfate, 10% fetal bovine serum, 1.5 µg/mL
489 cholesterol, 40 ng/mL M-CSF, 20 ng/mL GM-CSF, and 2 ng/mL TGF-β) adapted from [Bohlen et
490 al., 2017].

491

492 Microglia *in vitro* Phagocytosis Assay

493 The phagocytosis assay was performed using live cell imaging by Incucyte S3 (Essen BioScience)
494 for WB or SVZ microglia phagocytosis from 3- or 12-month mice. WB microglia were passaged
495 from a 6-well plate with Trypsin (Fisher, Cat. No. 25-200-072) following MACS isolation and
496 SVZ microglia were collected from mixed glial culture and microglia were plated in a 96 well
497 plate coated with PLO/laminin at 20k cells/well in microglia expansion media for 3 days. After 3
498 days, SVZ and WB microglia were moved to serum free media (DMEM/F12, 100 µg/mL PenStrep,
499 5 µg/mL n-acetyl-L-cysteine, 5 µg/mL Insulin, 100 µg/mL apo-transferrin, 100 µg/mL sodium
500 selenite, 1 µg/mL heparin sulfate, 1.5 µg/mL cholesterol, 40 ng/mL M-CSF, and 2 ng/mL TGF-β)
501 adapted from [Bohlen et al., 2017] for 1 week. All microglia were then incubated with 5 µg/mL
502 Isolectin IB4 Alexa Fluor™ 488 Conjugate (Invitrogen, Cat. No. I21411) for 60 minutes at 37°C.
503 SVZ or WB microglia of both ages were treated with Zymosan S. cerevisiae BioParticles™ (10
504 mg/mL; Invitrogen, Cat. No. Z2849) conjugated pHrodo™ Red SE (Molecular Probes™, Cat. No.
505 P36600) following manufacturer protocols (ThermoFisher) and adapted from [Haney et al., 2018;
506 Pluvinage et al., 2019], both Zymosan-pHrodo and Cytochalasin D (10 mM/µL Sigma-aldrich,
507 Cat. No. C8273) to inhibit phagocytosis, or isolectin only as a negative control. The microglia
508 were then incubated in the Incucyte S3 with fluorescent images captured every hour over the
509 course of 48 hours for live cell imaging of microglia phagocytosis. The images were analyzed in
510 the IncuCyte software (Essen BioScience) quantifying colocalization of the green fluorescence of

511 Isolectin IB4 labelled microglia and the red fluorescence of engulfed Zymosan-pHrodo within the
512 microglia lysosome demonstrating microglia phagocytosis. Total pHrodo area / number of
513 microglia was calculated for each well and condition yielding amount of in vitro phagocytosis
514 occurring at each time point.

515

516 RNA Extraction and qPCR

517 RNA was extracted from freshly isolated microglia following magnetic-activated cell sorting
518 (MACS) isolation, using a TRIzol-chloroform method (Rio et al., 2010) where cells were lysed in
519 TRIzol (Invitrogen, Cat. No. 15596018), aqueous layer separated with chloroform, RNA was
520 precipitated with isopropanol, washed in ethanol, dried, then resuspended in RNase-free water.
521 cDNA was synthesized using High Capacity cDNA Reverse Transcription Kit (Applied
522 Biosystems, Cat. No. 4368814). Quantitative polymerase chain reaction (qPCR) was performed
523 using a C1000 Touch Thermal Cycler (BioRad) with iTaq™ Universal SYBR® Green Supermix
524 (BioRad, Cat. No. 1725121). Reactions were performed in doublet with glyceraldehyde-3-
525 phosphate dehydrogenase (GAPDH) used as an endogenous control. Negative control reactions
526 were performed using the same conditions without cDNA. Quantification was analyzed using the
527 ΔΔCt method as described [Livak and Schmittgen, 2001]. Primers were used for the following
528 transcripts: C1QA, P2Y12, TREM2, LPAR, C3, CR1, ITGAM, ITGAX, GAPDH.

Primers	Forward	Reverse
C1QA	AAAGGCAATCCAGGCAATATCA	TGGTTCTGGTATGGACTCTCC
C3	CCAGCTCCCCATTAGCTCTG	GCACTTGCCTCTTTAGGAAGTC

TREM2	CTGGAACCGTCACCATCACTC	CGAAACTCGATGACTCCTCGG
LPAR	AGCCATGAACGAACAACAGTG	CATGATGAACACGCAAACAGTG
CR1	ATGGAGGTCTCTTCTCGGAGT	GGCCGAAGGCTACAAGGAG
ITGAM	GGGAGGACAAAAACTGCCTCA	ACAACTAGGATCTTCGCAGCAT
ITGAX	CTGGATAGCCTTTCTTCTGCTG	GCACACTGTGTCCGAACTCA
GAPDH	AGGTCGGTGTGAACGGATTTG	TGTAGACCATGTAGTTGAGGTCA

529

530 EdU Labeling and Staining

531 Mice were injected intraperitoneally (50µg EdU/1g mouse) 2 hours before sacrifice. Their brains
532 were removed and SVZ was isolated and fixed for 30 minutes in 4% PFA. EdU staining was
533 performed following manufacturer protocols (Fisher, Click-it EdU Imaging Kit, Cat. No. C10337).

534

535 Data Analysis

536 Student's t-tests and two-way ANOVA were used to analyze the data on GraphPad Prism 8
537 Software. All data are expressed as mean ± standard error of the mean.

538

539 **Data Availability**

540 Normalized single-cell RNA-sequencing data and cell type annotations of the SVZ from young (3
541 months old) and old (28–29 months old) male mice (n = 3) was downloaded from Supplementary

542 Table 2 of the Dulken et al., 2019 study. Results of screen for phagocytosis regulator genes were
543 downloaded from Supplementary Table 5 of the Haney et al., 2019 study and Supplementary Table
544 2 of the Pluvinage et al., 2019 study. Marker genes of major cell types in the SVZ of young (2-4
545 months old) male and female mice were downloaded from Table S1 of the Zywitza et al., 2018
546 study.

547

548 **Code Availability**

549 Code to reproduce bioinformatics analyses are available at the following repository:
550 https://github.com/cutleraging/nsc-aging

551

552 **References**

553 Ahlenius, H., Visan, V., Kokaia, M., Lindvall, O., and Kokaia, Z. (2009). Neural stem and
554 progenitor cells retain their potential for proliferation and differentiation into functional neurons
555 despite lower number in aged brain. J. Neurosci. *29*, 4408–4419.
556 https://doi.org/10.1523/JNEUROSCI.6003-08.2009.

557 Alvarez-Buylla, A., and García-Verdugo, J.M. (2002). Neurogenesis in adult subventricular zone.
558 J. Neurosci. *22*, 629–634. https://doi.org/10.1523/jneurosci.22-03-00629.2002.

559 Atkinson, C., Song, H., Lu, B., Qiao, F., Burns, T.A., Holers, V.M., Tsokos, G.C., and Tomlinson,
560 S. (2005). Targeted complement inhibition by C3d recognition ameliorates tissue injury without
561 apparent increase in susceptibility to infection. J. Clin. Invest. *115*, 2444–2453.
562 https://doi.org/10.1172/JCI25208.

563 Colonna, M., and Butovsky, O. (2017). Microglia function in the central nervous system during
564 health and neurodegeneration. Annu. Rev. Immunol. *35*, 441–468.
565 https://doi.org/10.1146/annurev-immunol-051116-052358.

566 Elewa, H.F., Hilali, R., Hess, D.C., Machado, L.S., and Fagan, S.C. (2006). Minocycline for short-
567 term neuroprotection. Pharmacotherapy *26*, 515–521. https://doi.org/10.1592/phco.26.4.515.

568 Enwere, E., Shingo, T., Gregg, C., Fujikawa, H., Ohta, S., and Weiss, S. (2004). Aging results in
569 reduced epidermal growth factor receptor signaling, diminished olfactory neurogenesis, and
570 deficits in fine olfactory discrimination. J. Neurosci. *24*, 8354–8365.
571 https://doi.org/10.1523/JNEUROSCI.2751-04.2004.

572 Garrido-Mesa, N., Zarzuelo, A., and Gálvez, J. (2013). Minocycline: Far beyond an antibiotic. Br.
573 J. Pharmacol. *169*, 337–352. https://doi.org/10.1111/bph.12139.

574 Ginhoux, F., Greter, M., Leboeuf, M., Nandi, S., See, P., Gokhan, S., Mehler, M.F., Conway, S.J.,
575 Ng, L.G., Stanley, E.R., et al. (2010). Fate mapping analysis reveals that adult microglia derive
576 from primitive macrophages. Science (80-.). *330*, 841–845.
577 https://doi.org/10.1126/science.1194637.

578 Goings, G.E., Kozlowski, D.A., and Szele, F.G. (2006). Differential activation of microglia in
579 neurogenic versus non-neurogenic regions of the forebrain. Glia *54*, 329–342.
580 https://doi.org/10.1002/glia.20381.

581 Kalamakis, G., Brüne, D., Ravichandran, S., Bolz, J., Fan, W., Ziebell, F., Stiehl, T., Catalá-
582 Martinez, F., Kupke, J., Zhao, S., et al. (2019). Quiescence Modulates Stem Cell Maintenance and
583 Regenerative Capacity in the Aging Brain. Cell *176*, 1407-1419.e14.
584 https://doi.org/10.1016/j.cell.2019.01.040.

585 Kapellos, T.S., Taylor, L., Lee, H., Cowley, S.A., James, W.S., Iqbal, A.J., and Greaves, D.R.
586 (2016). A novel real time imaging platform to quantify macrophage phagocytosis. Biochem.
587 Pharmacol. *116*, 107–119. https://doi.org/10.1016/j.bcp.2016.07.011.

588 Kim, E.J., Ables, J.L., Dickel, L.K., Eisch, A.J., and Johnson, J.E. (2011). Ascl1 (Mash1) Defines
589 Cells with Long-Term Neurogenic Potential inSubgranular and Subventricular Zones in Adult
590 Mouse Brain. PLoS One *6*, 18472. https://doi.org/10.1371/JOURNAL.PONE.0018472.

591 Lim, D.A., and Alvarez-Buylla, A. (2016). The adult ventricular–subventricular zone (V-SVZ)
592 and olfactory bulb (OB) neurogenesis. Cold Spring Harb. Perspect. Biol. *8*, a018820.
593 https://doi.org/10.1101/cshperspect.a018820.

594 Marshall, G.P., Deleyrolle, L.P., Reynolds, B.A., Steindler, D.A., and Laywell, E.D. (2014).
595 Microglia from neurogenic and non-neurogenic regions display differential proliferative potential
596 and neuroblast support. Front. Cell. Neurosci. *8*, 180. https://doi.org/10.3389/fncel.2014.00180.

597 Maslov, A.Y., Barone, T.A., Plunkett, R.J., and Pruitt, S.C. (2004). Neural Stem Cell Detection,
598 Characterization, and Age-Related Changes in the Subventricular Zone of Mice. J. Neurosci. *24*,
599 1726–1733. https://doi.org/10.1523/JNEUROSCI.4608-03.2004.

600 Plane, J.M., Shen, Y., Pleasure, D.E., and Deng, W. (2010). Prospects for minocycline
601 neuroprotection. Arch. Neurol. *67*, 1442–1448. https://doi.org/10.1001/archneurol.2010.191.

602 Ribeiro Xavier, A.L., Kress, B.T., Goldman, S.A., De Lacerda Menezes, J.R., and Nedergaard, M.
603 (2015). A distinct population of microglia supports adult neurogenesis in the subventricular zone.
604 J. Neurosci. *35*, 11848–11861. https://doi.org/10.1523/JNEUROSCI.1217-15.2015.

605 Shigemoto-Mogami, Y., Hoshikawa, K., Goldman, J.E., Sekino, Y., and Sato, K. (2014).

606 Microglia enhance neurogenesis and oligodendrogenesis in the early postnatal subventricular
607 zone. J. Neurosci. *34*, 2231–2243. https://doi.org/10.1523/JNEUROSCI.1619-13.2014.

608 Solano Fonseca, R., Mahesula, S., Apple, D.M., Raghunathan, R., Dugan, A., Cardona, A.,
609 O'Connor, J., and Kokovay, E. (2016). Neurogenic niche microglia undergo positional remodeling
610 and progressive activation contributing to age-associated reductions in neurogenesis. Stem Cells
611 Dev. *25*, 542–555. https://doi.org/10.1089/scd.2015.0319.

612 Song, H., He, C., Knaak, C., Guthridge, J.M., Holers, V.M., and Tomlinson, S. (2003).
613 Complement receptor 2-mediated targeting of complement inhibitors to sites of complement
614 activation. J. Clin. Invest. *111*, 1875–1885. https://doi.org/10.1172/JCI17348.

615 Tikka, T., Fiebich, B.L., Goldsteins, G., Keinänen, R., and Koistinaho, J. (2001). Minocycline, a
616 tetracycline derivative, is neuroprotective against excitotoxicity by inhibiting activation and
617 proliferation of microglia. J. Neurosci. *21*, 2580–2588. https://doi.org/10.1523/jneurosci.21-08-
618 02580.2001.

619 Yrjänheikki, J., Keinänen, R., Pellikka, M., Hökfelt, T., and Koistinaho, J. (1998). Tetracyclines
620 inhibit microglial activation and are neuroprotective in global brain ischemia. Proc. Natl. Acad.
621 Sci. U. S. A. *95*, 15769–15774. https://doi.org/10.1073/pnas.95.26.15769.

622

623

624 Cunningham, C. L., Martínez-Cerdeño, V., & Noctor, S. C. (2013). Microglia Regulate the Number
625 of Neural Precursor Cells in the Developing Cerebral Cortex.
626 https://doi.org/10.1523/JNEUROSCI.3441-12.2013

627 Deczkowska, A., Keren-Shaul, H., Weiner, A., Colonna, M., Schwartz, M., & Amit, I. (2018).
628 Disease-Associated Microglia: A Universal Immune Sensor of Neurodegeneration. In A.
629 W. Hadas Keren-Shaul 1 2 5, Marco Colonna 3, Michal Schwartz 4, Ido Amit 1 (Ed.). Cell.
630 G, Y., LG, W., Y, H., & QY, H. (2012). clusterProfiler: an R package for comparing biological
631 themes among gene clusters. *Omics : a journal of integrative biology*, *16*(5).
632 https://doi.org/10.1089/omi.2011.0118
633 Haney, M. S., Bohlen, C. J., Morgens, D. W., Ousey, J. A., Barkal, A. A., Tsui, C. K., Ego, B. K.,
634 Levin, R., Kamber, R. A., Collins, H., Tucker, A., Li, A., Vorselen, D., Labitigan, L., Crane,
635 E., Boyle, E., Jiang, L., Chan, J., Rincón, E., . . . Bassik, M. C. (2018). Identification of
636 phagocytosis regulators using magnetic genome-wide CRISPR screens. *Nat Genet*, *50*(12),
637 1716-1727. https://doi.org/10.1038/s41588-018-0254-1
638 Hu, B., Fujian Provincial Key Laboratory of Neurodegenerative Disease and Aging Research, S.
639 o. M., Institute of Neuroscience, Xiamen University, Xiamen, China, Duan, S., Fujian
640 Provincial Key Laboratory of Neurodegenerative Disease and Aging Research, S. o. M.,
641 Institute of Neuroscience, Xiamen University, Xiamen, China, Wang, Z., Fujian Provincial
642 Key Laboratory of Neurodegenerative Disease and Aging Research, S. o. M., Institute of
643 Neuroscience, Xiamen University, Xiamen, China, Li, X., Fujian Provincial Key
644 Laboratory of Neurodegenerative Disease and Aging Research, S. o. M., Institute of
645 Neuroscience, Xiamen University, Xiamen, China, Zhou, Y., Fujian Provincial Key
646 Laboratory of Neurodegenerative Disease and Aging Research, S. o. M., Institute of
647 Neuroscience, Xiamen University, Xiamen, China, Zhang, X., Fujian Provincial Key
648 Laboratory of Neurodegenerative Disease and Aging Research, S. o. M., Institute of
649 Neuroscience, Xiamen University, Xiamen, China, Zhang, Y.-W., Fujian Provincial Key

650 Laboratory of Neurodegenerative Disease and Aging Research, S. o. M., Institute of
651 Neuroscience, Xiamen University, Xiamen, China, Xu, H., Fujian Provincial Key
652 Laboratory of Neurodegenerative Disease and Aging Research, S. o. M., Institute of
653 Neuroscience, Xiamen University, Xiamen, China, Zheng, H., Fujian Provincial Key
654 Laboratory of Neurodegenerative Disease and Aging Research, S. o. M., Institute of
655 Neuroscience, Xiamen University, Xiamen, China, & Basic Medical Sciences, S. o. M.,
656 Xiamen University, Xiamen, China. (2024). Insights Into the Role of CSF1R in the Central
657 Nervous System and Neurological Disorders. *Frontiers in Aging Neuroscience*, *13*,
658 789834. https://doi.org/10.3389/fnagi.2021.789834

659 Izgi, H., Han, D., Isildak, U., Huang, S., Kocabiyik, E., Khaitovich, P., Somel, M., & Dönertaş, H.
660 M. (2022). Inter-tissue convergence of gene expression during ageing suggests age-related
661 loss of tissue and cellular identity. https://doi.org/doi:10.7554/eLife.68048

662 Khalaji, A., Yancheshmeh, F. B., Farham, F., Khorram, A., Sheshbolouki, S., Zokaei, M.,
663 Vatankhah, F., & Soleymani-Goloujeh, M. (2023). Don't eat me/eat me signals as a novel
664 strategy in cancer immunotherapy. *Heliyon*, *9*(10), e20507.
665 https://doi.org/10.1016/j.heliyon.2023.e20507

666 Li, W. (2012). Eat-me signals: keys to molecular phagocyte biology and "appetite" control. *J Cell*
667 *Physiol*, *227*(4), 1291-1297. https://doi.org/10.1002/jcp.22815

668 Liberzon, A., Broad Institute of MIT and Harvard, M. S. C., MA 02142, USA, Birger, C., Broad
669 Institute of MIT and Harvard, M. S. C., MA 02142, USA, Thorvaldsdóttir, H., Broad
670 Institute of MIT and Harvard, M. S. C., MA 02142, USA, Ghandi, M., Broad Institute of
671 MIT and Harvard, M. S. C., MA 02142, USA, Mesirov, J. P., Broad Institute of MIT and
672 Harvard, M. S. C., MA 02142, USA, Department of Medicine, U. S. D., La Jolla, CA

673 92093, USA, Moores Cancer Center, U. S. D., La Jolla, CA 92093, USA, Tamayo, P., Broad
674 Institute of MIT and Harvard, M. S. C., MA 02142, USA, Department of Medicine, U. S.
675 D., La Jolla, CA 92093, USA, & Moores Cancer Center, U. S. D., La Jolla, CA 92093,
676 USA. (2024). The Molecular Signatures Database (MSigDB) hallmark gene set collection.
677 *Cell systems*, *1*(6), 417. https://doi.org/10.1016/j.cels.2015.12.004
678 Luo, J., SB, D., JB, L., RQ, N., & JC, C. (2006). The aging neurogenic subventricular zone. *Aging*
679 *cell*, *5*(2). https://doi.org/10.1111/j.1474-9726.2006.00197.x
680 MI, L., W, H., & S, A. (2014). Moderated estimation of fold change and dispersion for RNA-seq
681 data with DESeq2. *Genome biology*, *15*(12). https://doi.org/10.1186/s13059-014-0550-8
682 Pluvinage, J. V., Haney, M. S., Smith, B. A. H., Sun, J., Iram, T., Bonanno, L., Li, L., Lee, D. P.,
683 Morgens, D. W., Yang, A. C., Shuken, S. R., Gate, D., Scott, M., Khatri, P., Luo, J.,
684 Bertozzi, C. R., Bassik, M. C., & Wyss-Coray, T. (2019). CD22 blockade restores
685 homeostatic microglial phagocytosis in ageing brains. *Nature*, *568*(7751), 187-192.
686 https://doi.org/10.1038/s41586-019-1088-4
687 Sierra, A., JM, E., JJ, D., JH, C., G, E., LS, O.-W., SE, T., & M, M.-S. (2010). Microglia shape
688 adult hippocampal neurogenesis through apoptosis-coupled phagocytosis. *Cell stem cell*,
689 *7*(4). https://doi.org/10.1016/j.stem.2010.08.014
690 Solano, F., S, M., DM, A., R, R., A, D., A, C., J, O. C., & E, K. (2016). Neurogenic Niche Microglia
691 Undergo Positional Remodeling and Progressive Activation Contributing to Age-
692 Associated Reductions in Neurogenesis. *Stem cells and development*, *25*(7).
693 https://doi.org/10.1089/scd.2015.0319
694 Xavier, A. R., BT, K., SA, G., JR, L. d. M., & M, N. (2015). A Distinct Population of Microglia
695 Supports Adult Neurogenesis in the Subventricular Zone. *The Journal of neuroscience :*

696 *the official journal of the Society for Neuroscience*, *35*(34).
697 https://doi.org/10.1523/JNEUROSCI.1217-15.2015
698 Yen, J.-H. J., Department of Microbiology and Immunology, I. U. S. o. M., Indianapolis, IN, USA,
699 Yu, I.-C. I., & Department of Anatomy, C. B., and Physiology, Indiana University School
700 of Medicine, Fort Wayne, IN, USA. (2024). The role of ApoE-mediated microglial lipid
701 metabolism in brain aging and disease. *Immunometabolism (Cobham (Surrey, England)*,
702 *5*(1). https://doi.org/10.1097/IN9.0000000000000018

703

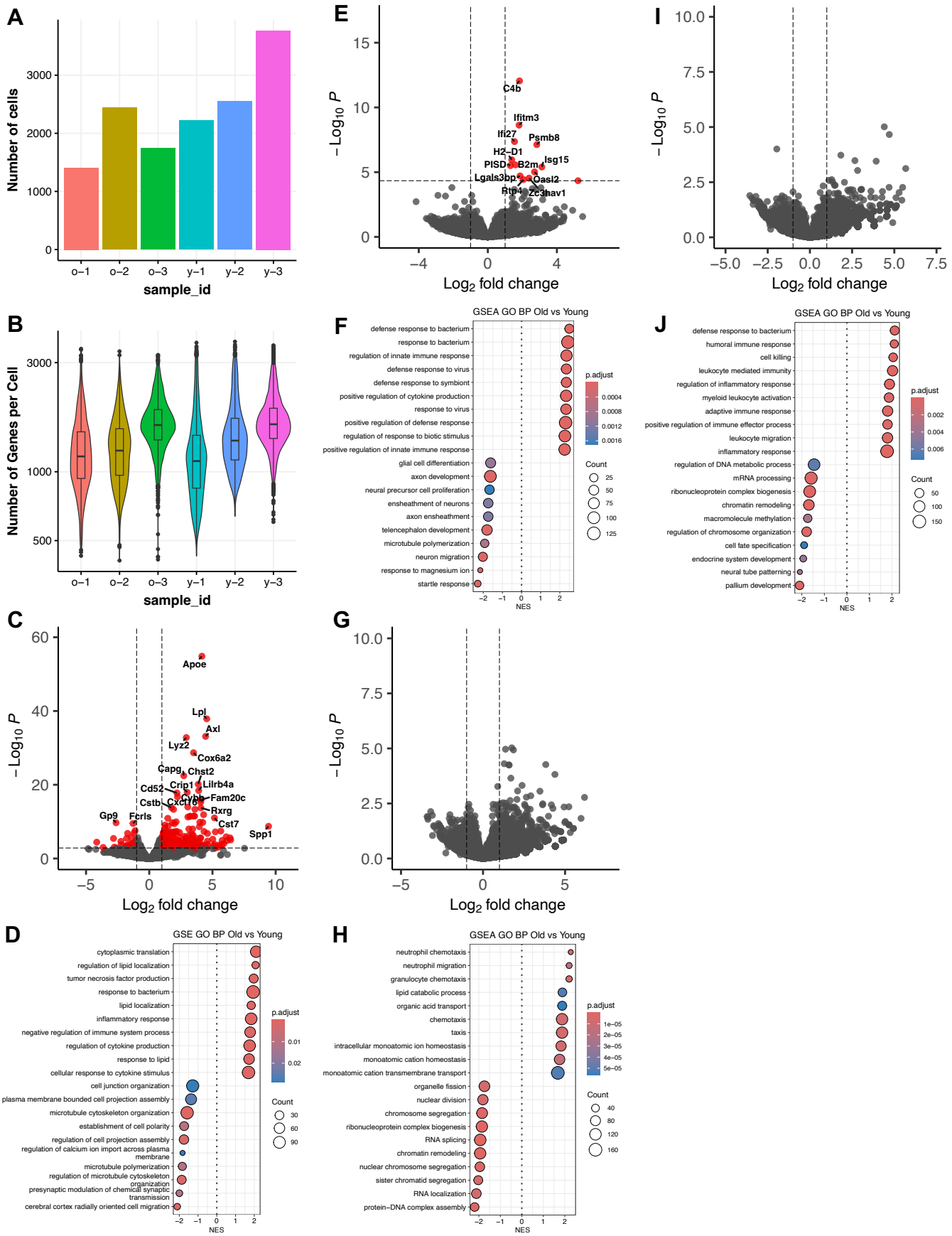

Supplementary Figure 1. Quality control, differential expression, and gene set enrichment analysis of major cell types in Dulken *et al*., 2019 aging SVZ scRNA dataset

A) Number of cells captured per sample. O=old (28-29 months old) and Y=young (3 months old), number indicates mouse replicate. B) Distribution of genes identified per cell in each sample. C) SVZ microglia pseudobulk differential gene expression of old vs. young. Red points are $\log_2$ fold change > 1 and adjusted p-value < 0.05. Statistics: n=3 mice/group, DGE results obtained using Wald test followed by Benjamini-Hochberg correction for multiple hypothesis testing. D) SVZ microglia gene set enrichment analysis of gene ontology biological process for old vs. young differentially expressed genes shown in (C). Statistics: GSEA p-values obtained using a permutation test followed by followed by Benjamini-Hochberg correction for multiple hypothesis testing. E-F) Same as in B-C, but for astrocytes-quiescent neural stem cells (qNSCs). G-H) Same as in B-C, but for activate neural stem cells (aNSCs) – neural progenitor cells (NPCs). I-J) Same as in B-C, but for neuroblasts.

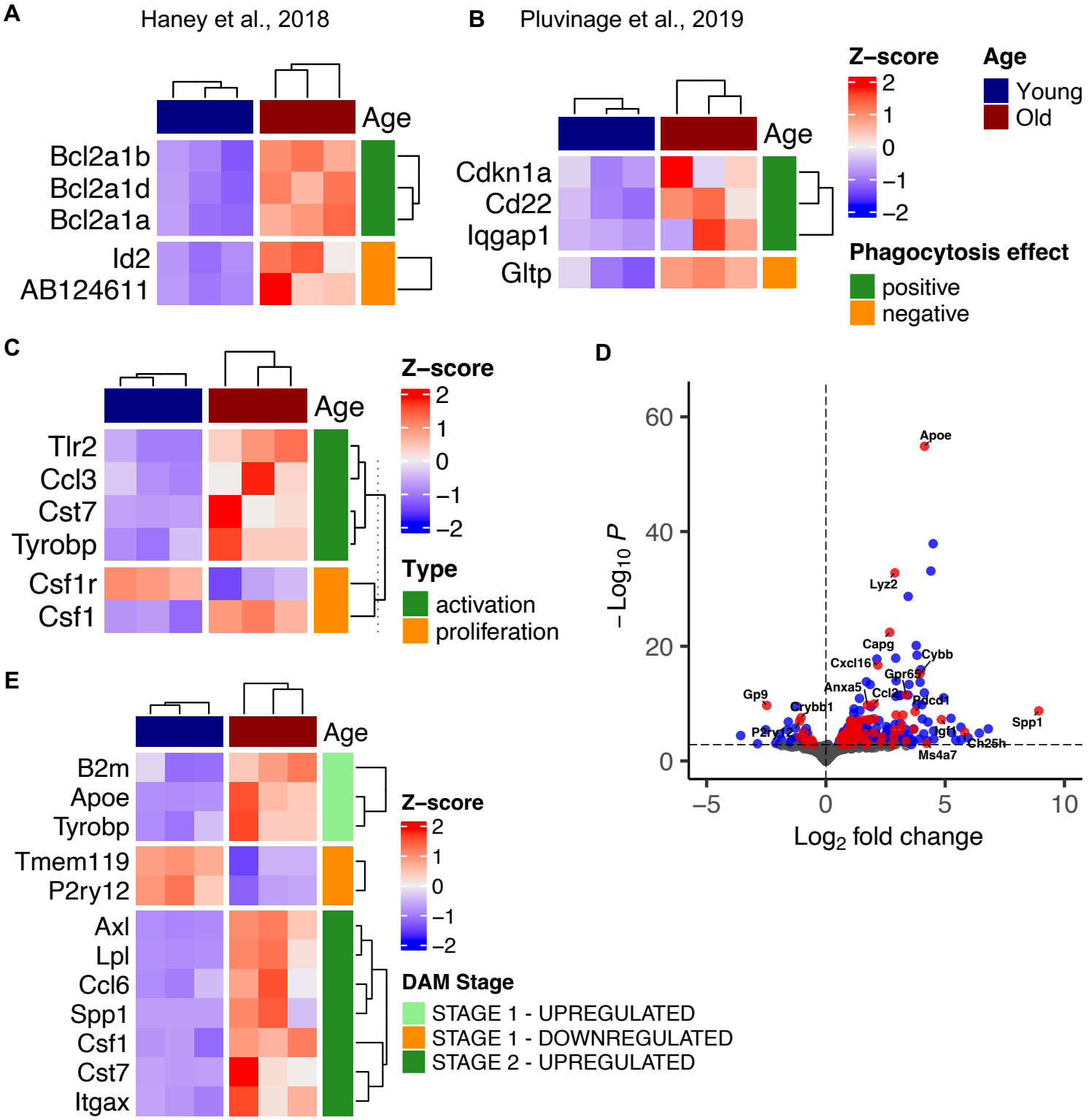

Supplementary Figure 2. Extended analysis of aging SVZ microglia gene expression changes

A-B) Heatmap of age-related differentially expressed genes (ARDEGs; adjusted p-value < 0.05) in aging SVZ microglia that overlapped with gene sets derived from screens to identify genes regulating phagocytosis from Haney *et al*., 2018 (A) and Pluvinage *et al*., 2019 (B). Statistics: n=3 mice/group C) Same as in (A), but for ARDEGs that overlapped with the Molecular Signatures Database MICROGLIAL CELL ACTIVATION or MICROGLIAL CELL PROLIFERATION gene sets (Supplementary Table 2). D) SVZ microglia pseudobulk differential gene expression of old vs. young where points highlighted in red are genes that are $\log_2$ fold change > 1 and adjusted p-value < 0.05 and that overlapped with the Molecular Signatures Database entries: DESCARTES FETAL CEREBELLUM MICROGLIA, DESCARTES FETAL CEREBRUM MICROGLIA, DESCARTES MAIN FETAL MICROGLIA, FAN EMBRYONIC CTX BIG GROUPS MICROGLIA, FAN EMBRYONIC CTX MICROGLIA 1,FAN EMBRYONIC CTX MICROGLIA 2, FAN EMBRYONIC CTX MICROGLIA 3 gene sets (Supplementary Table 2). Statistics: n=3 mice/group. E) Same as in (A), but for ARDEGs that overlapped with the disease associated microglia (DAM) gene sets reviewed in Deczkowska *et al*., 2018 (Supplementary Table 2).

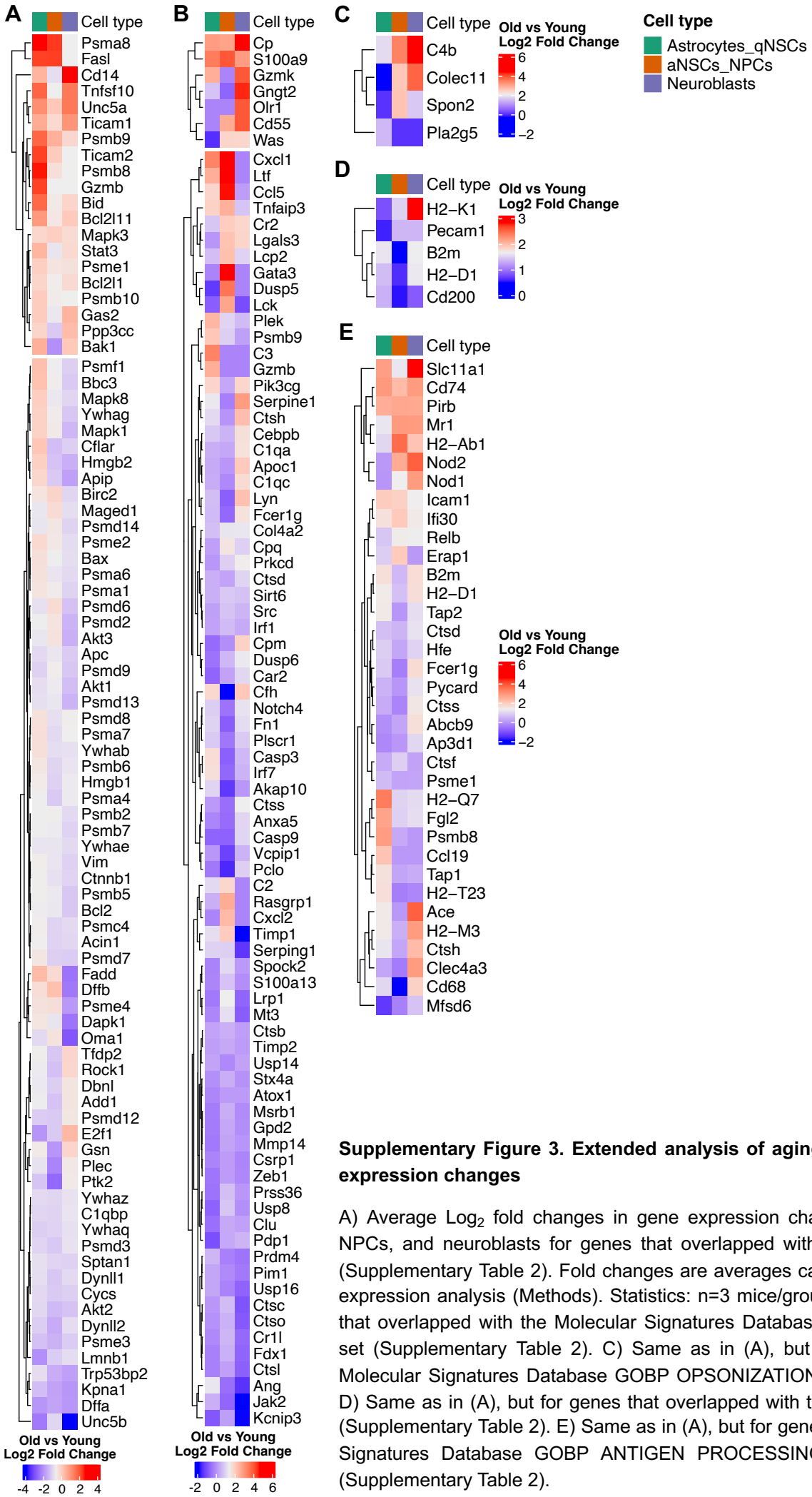

Supplementary Figure 3. Extended analysis of aging SVZ neural progenitor cell gene expression changes

A) Average Log_2 fold changes in gene expression changes for astrocytes-qNSC, aNSCs-NPCs, and neuroblasts for genes that overlapped with the Reactome Apoptosis gene set (Supplementary Table 2). Fold changes are averages calculated form pseudobulk differential expression analysis (Methods). Statistics: n=3 mice/group. B) Same as in (A), but for genes that overlapped with the Molecular Signatures Database HALLMARK COMPLEMENT gene set (Supplementary Table 2). C) Same as in (A), but for genes that overlapped with the Molecular Signatures Database GOBP OPSONIZATION gene set (Supplementary Table 2). D) Same as in (A), but for genes that overlapped with the curated DON'T EAT ME gene set (Supplementary Table 2). E) Same as in (A), but for genes that overlapped with the Molecular Signatures Database GOBP ANTIGEN PROCESSING AND PRESENTATION gene set (Supplementary Table 2).

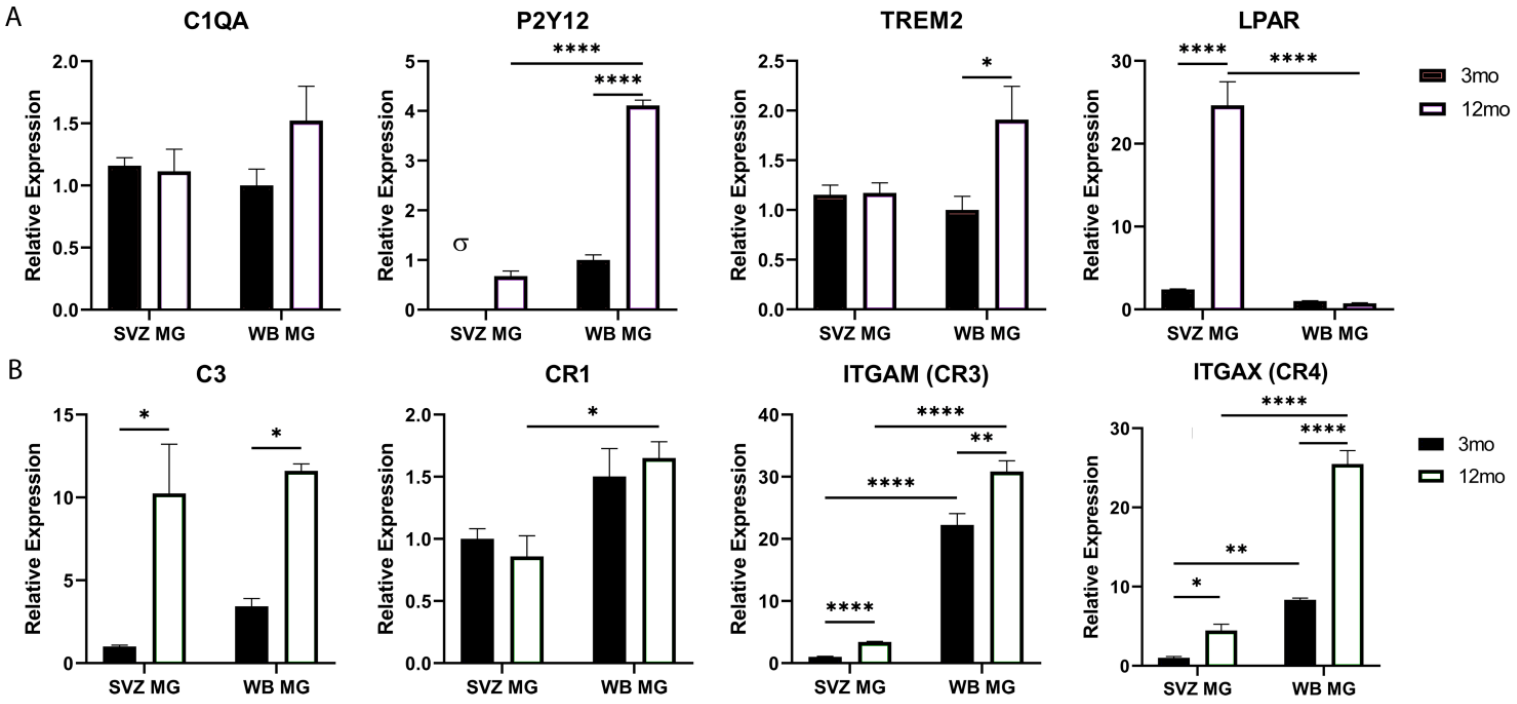

Supplementary Figure 4. qPCR validation of genes selected from the scRNA-Seq results
(A-B) Quantification of gene expression of microglia from the SVZ (SVZ MG) or whole brain (WB MG) in young (3 months) and aged (12 months) mice. Statistics: n=3 mice/group; σ: not detected. P-value legend: ns: no symbol; *: p ≤ 0.05, **: p ≤ 0.01, ***: p ≤ 0.001, ****: p ≤ 0.0001.